High-Magnitude and/or High-Frequency Mechanical Strain Promotes Peripapillary Scleral Myofibroblast Differentiation

Jing Qu,[1] Huaping Chen,[1] Lanyan Zhu,[1,2] Namasivayam Ambalavanan,[3] Christopher A. Girkin,[4] Joanne E. Murphy-Ullrich,[4,5] J. Crawford Downs,[4,6] and Yong Zhou[1,4,6]

[1]Department of Medicine, University of Alabama at Birmingham, Birmingham, Alabama, United States
[2]The Second Xiangya Hospital, Central-South University, Changsha, Hunan, China
[3]Department of Pediatrics, University of Alabama at Birmingham, Birmingham, Alabama, United States
[4]Department of Ophthalmology, University of Alabama at Birmingham, Birmingham, Alabama, United States
[5]Department of Pathology, University of Alabama at Birmingham, Birmingham, Alabama, United States
[6]Department of Biomedical Engineering, University of Alabama at Birmingham, Birmingham, Alabama, United States

Correspondence: Yong Zhou, Departments of Medicine, Ophthalmology, and Biomedical Engineering, Tinsley Harrison Tower 437B, 1900 University Boulevard, Birmingham, AL 35294, USA; yzhou@uab.edu.

Submitted: July 31, 2015
Accepted: November 10, 2015

Citation: Qu J, Chen H, Zhu L, et al. High-magnitude and/or high-frequency mechanical strain promotes peripapillary scleral myofibroblast differentiation. *Invest Ophthalmol Vis Sci*. 2015;56:7821–7830. DOI:10.1167/iovs.15-17848

Purpose. To determine the effects of altered mechanical strain on human peripapillary scleral (ppSc) fibroblast-to-myofibroblast differentiation.

Methods. Eight human ppSc fibroblast cultures were isolated from three paired eyes and two unilateral eyes of five donors using an explant approach. Human ppSc fibroblast isolates were subjected to 1% and 4% cyclic strain at 0.05 to 5 Hz for 24 hours. Levels of α smooth muscle actin (αSMA) mRNA and protein were determined by real-time PCR and immunoblot. Incorporation of αSMA into actin stress fibers was evaluated by confocal immunofluorescent microscopy. Myofibroblast contractility was measured by fibroblast-populated three-dimensional collagen gel contraction assay and phosphorylation of myosin light chain (MLC_{20}).

Results. Human ppSc fibroblasts contained 6% to 47% fully differentiated myofibroblasts before strain application; 4% cyclic strain increased αSMA mRNA and protein expression in ppSc fibroblasts compared with 1% strain applied at 5 Hz, but not at lower frequencies. Seven of eight ppSc fibroblast isolates responded to high-magnitude and high-frequency strain with increased cellular contractility and increased MLC_{20} phosphorylation. In addition, increasing strain frequency promoted αSMA expression in ppSc fibroblasts under both 1% and 4% strain conditions.

Conclusions. High-magnitude and/or high-frequency mechanical strain promotes differentiation of human ppSc fibroblasts into contractile myofibroblasts, a fibroblast phenotypic change known to be key to tissue injury–repair responses. These findings suggest that the cellular constituent of ppSc may play an important role in the regulation of optic nerve head biomechanics in response to injurious IOP fluctuations.

Keywords: peripapillary sclera, fibroblast, myofibroblast, mechanical strain, glaucoma

Deformation of the load-bearing tissues of the optic nerve head (ONH) due to IOP-generated stress is believed to play an important role in the pathogenesis of glaucomatous optic neuropathy.[1–3] The peripapillary sclera (ppSc) provides mechanical boundary conditions of the ONH at the neural canal and transmits biomechanical strain directly to the lamina cribrosa (LC) at its insertion into the scleral canal wall. Hence, the IOP-related biomechanical response of the ppSc plays a crucial role in the regulation of biomechanical response and environment of the ONH and LC.[4–6] Histomorphometric and computational modeling studies provide evidence that both the material properties and geometry of the ppSc, which are altered in glaucomatous eyes of both human patients and experimental nonhuman primates,[7–11] significantly impact the scleral canal and LC deformations in response to IOP variation.[12–16] These findings suggest that the material properties and geometry of the ppSc are determinants of the mechanical environment at the ONH.

Mechanical strain induced by IOP not only alters the physical properties of load-bearing sclera, but activates the cells residing within the sclera that can in turn alter the material properties and geometry of the sclera through production of extracellular matrix (ECM) proteins and secretion of connective tissue remodeling factors, including matrix metalloproteinases (MMPs) and tissue inhibitors of metalloproteinases (TIMPs).[17–19] In most mammalian species, fibroblasts are the primary cells found in sclera, although chondrocytes have been reported in the inner cartilaginous layer of sheep.[20] In vivo assessments of scleral creep response in tree shrew eyes versus chick eyes suggest that specialized contractile fibroblasts, known as myofibroblasts, play an important role in defining the mechanical properties of sclera.[21] Myofibroblasts are effector cells that drive connective tissue remodeling in the tissue injury–repair process.[22] These cells are absent in most adult tissues under normal conditions, but can be differentiated from various progenitor cells, including fibroblasts, during

tissue repair and remodeling processes.[22] The sclera of adult human, monkey, tree shrew, and guinea pig has been found to contain an endogenous population of myofibroblasts.[21,23,24] Although the origin and function of scleral myofibroblasts remain to be determined, it is thought that the presence of permanent scleral myofibroblasts might be a result of constant IOP-related strain, and that scleral myofibroblasts might work with collagen and other ECM components to resist the tensile effects of IOP on the eye. Myofibroblasts are activated fibroblasts that produce increased amounts of ECM proteins and ECM-regulating factors compared with their dormant progenitors.[25] However, unlike fibroblasts, myofibroblasts develop a significant capacity for contractile force through expressing a variety of actomyosin components, including α smooth muscle actin (αSMA),[26] making myofibroblasts capable of rapidly responding to imposed tissue stress, limiting expansion of the surrounding ECM. Because of the significant contractile potential, the number of myofibroblasts present in the ppSc would be expected to play a key role in biomechanical responses of the posterior sclera as well as the level of tensile stress applied on the ONH. The purpose of this study was to determine the effects of altered mechanical strain on human ppSc fibroblast-to-myofibroblast differentiation.

Methods

Peripapillary Sclera Fibroblast Isolation and Culture

Eight human eyes (three paired eyes and two unilateral eyes from five donors) from donors, without a history of ocular disease other than cataract, defined by family interview and medical records review, were obtained from the Alabama EyeBank. Consent was obtained for using the eyes for research purposes. The ppSc, a 2-mm-wide scleral band that surrounds the ONH, was carefully dissected and explanted from donor eyes received within 6 hours post mortem. Explanted tissue pieces were placed in 60-mm tissue culture dishes containing RPMI-1640 medium, 20% fetal bovine serum (FBS), 1% penicillin/streptomycin/glutamine, nonessential amino acids, and sodium pyruvate. Medium was replenished every 3 days. After 14 days, cells growing out of the explants were trypsinized and plated in Dulbecco's modified Eagle's medium (DMEM) with 10% FBS, 1% penicillin/streptomycin/glutamine, nonessential amino acids, and sodium pyruvate (supplemented DMEM). Fibroblasts of ppSc were used between passages 6 and 10.

Mechanical Stretch

Human ppSc fibroblasts (1.6×10^5/well) were seeded into 35-mm 6-well Bioflex collagen I-coated stretch plates (Flexcell Int. Corp., Hillsborough, NC, USA) in FBS-supplemented DMEM and incubated at 37°C for 6 hours to allow cell attachment. Cells were serum-starved in DMEM with 1% penicillin/streptomycin/glutamine for 24 hours. After replacement with serum-free media, ppSc fibroblasts were subjected to 1% or 4% cyclic stretch at 0.05 Hz, 0.5 Hz, and 5 Hz for 24 hours on a Flexcell FX-5000T Tension system. The strain magnitudes used in this study were based on the low and high range of values we measured in posterior scleral shells from human donors that were subjected to inflation tests (5–45 mm Hg).[27] The strain frequencies were based on our previous work showing that high-frequency IOP fluctuations are a common feature in nonhuman primates.[18] Given the similarities between humans and nonhuman primates, we assume that human eyes are subjected to similar levels of IOP spikes in vivo. Immediately after stretching was completed, Trizol reagent (Invitrogen, Carlsbad, CA, USA) was directly added on cells in Bioflex plates to extract total RNA. Radioimmunoprecipitation assay lysis buffer containing protease inhibitor cocktail and phosphatase inhibitor was added to cells in separate wells for extract proteins.

Real-Time RT-PCR

Total RNA was extracted with Trizol reagent (Invitrogen) according to the manufacturer's protocol, and 1 μg total RNA was reversely transcribed into cDNA with a cDNA Synthesis Kit (Bio-Rad Laboratories, Inc., Hercules, CA, USA). Real-time RT-PCR was performed using iQ SYBR Green PCR Supermix (Bio-Rad Laboratories, Inc.) on a LightCycler 480 (Roche Applied Science, Indianapolis, IN, USA). After an initial incubation at 95°C for 5 minutes, reaction mixtures were subjected to 40 cycles of amplification under the following conditions: 94°C for 15 seconds, 55°C for 15 seconds, and 72°C for 20 seconds. Specific PCR primers are: αSMA 5′-GACCGAATGCAGAAGGAGAT-3′ and 5′-CCACCGATCCAGACAGAGTA-3′; 18S rRNA (internal reference control) 5′-GTAACCCGTTGAACCCCATT-3′ and 5′-CCATCCAATCGGTAGTAGCG-3′. Each sample was run in triplicate; threshold cycles (CT) were averaged and normalized to endogenous 18S rRNA. The relative amount of amplified product was calculated using the comparative CT method.

Western Blot and Densitometry Analyses

Cell lysates containing 5 μg total proteins were resolved on 12% SDS-PAGE gels under reducing conditions. After electrophoresis, proteins were transferred to nitrocellulose membranes at 100 V for 1 hour at 4°C. Membranes were blocked with PBS containing 5% fat-free milk and 0.1% Tween 20 for 1 hour, and incubated with anti-αSMA antibody (American Research Products, Waltham, MA, USA), antiphospho myosin light chain $(MLC)_{20}$ antibody or anti-MLC_{20} antibody (Cell Signaling, Danvers, MA, USA), or anti–glyceraldehyde 3-phosphate dehydrogenase (GAPDH) antibody (Santa Cruz Biotechnology, Santa Cruz, CA, USA) for 2 hours followed by horseradish peroxidase–conjugated secondary antibody for 1 hour. Specific antigen-antibody reactions were detected by chemiluminescence. Images were scanned and bands were quantified by ImageJ (http://imagej.nih.gov/ij/; provided in the public domain by the National Institutes of Health, Bethesda, MD, USA). Fold increases or decreases in αSMA, phosphorylated MLC_{20} ($pMLC_{20}$), and total MLC_{20} protein were normalized to GAPDH protein.

Immunofluorescence and Confocal Laser Scanning Microscopy

Immunofluorescent staining and confocal laser scanning microscopy were performed as described in our previous studies.[28,29] Briefly, cells in Bioflex plates were fixed in 4% paraformaldehyde in PBS for 20 minutes and permeabilized with 0.5% Triton X-100 in PBS for 10 minutes. Cells were incubated with anti-αSMA antibody at room temperature for 1 hour followed by fluorescein isothiocyanate-conjugated secondary antibody for 1 hour. Then, cells were incubated with rhodamine-conjugated phalloidin at room temperature for 1 hour. Nuclei were stained with 4′,6-diamidino-2-phenylindole (DAPI). Stained cells and Bioflex membranes were removed from the plates with a scissor, placed on glass slides, and covered with coverslips. Fluorescent signals were detected using an inverted confocal laser scanning microscope Zeiss

Investigative Ophthalmology & Visual Science

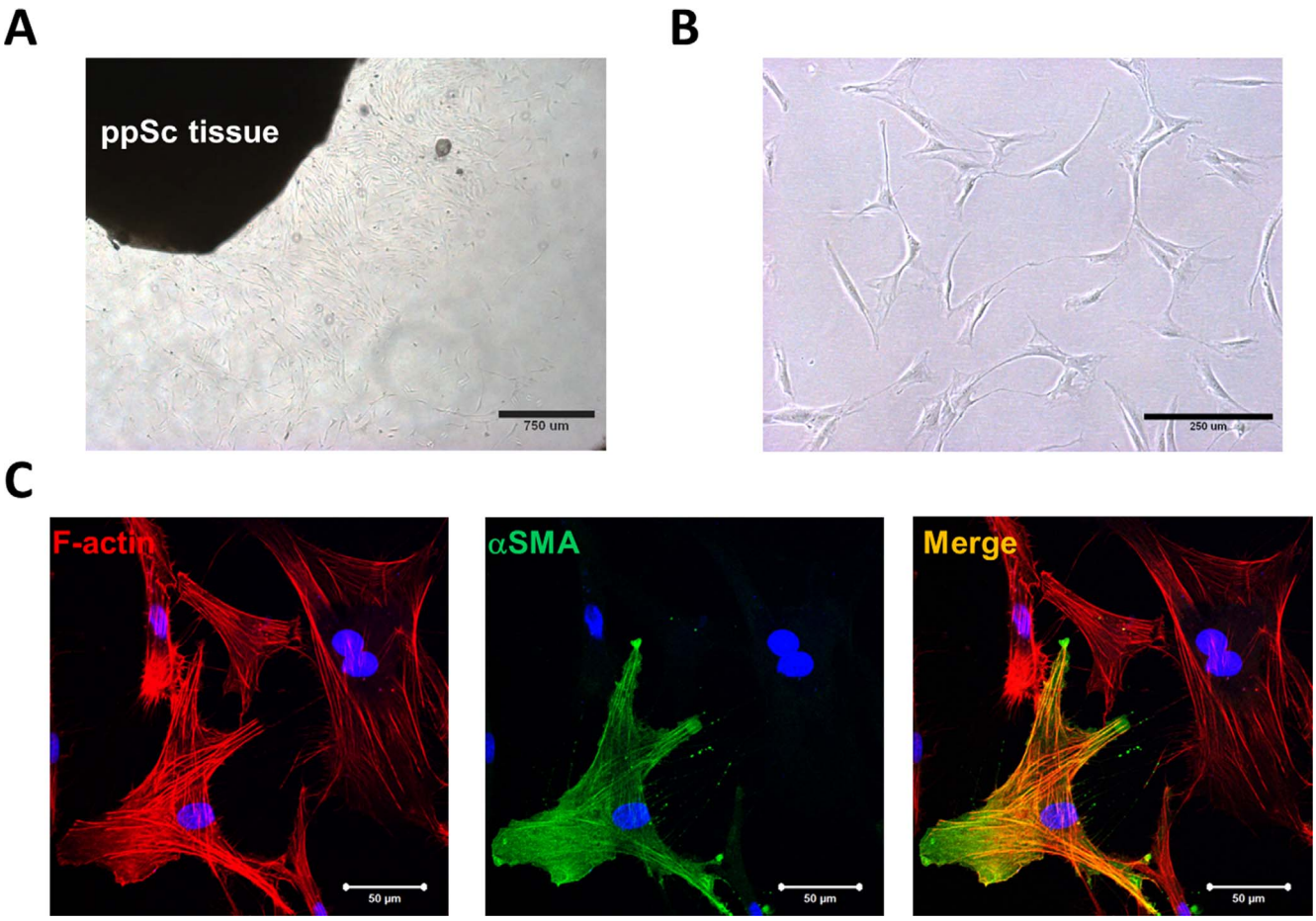

FIGURE 1. Isolation of human primary ppSc fibroblasts and identification of endogenous ppSc myofibroblast population. (**A**) Migration of fibroblasts from a human ppSc tissue explant. (**B**) Morphology of human ppSc fibroblasts at passage 3. (**C**) Human ppSc fibroblasts at passage 3 were stained for αSMA (*green*) and F-actin (*red*). Nuclei were stained by DAPI (*blue*). *Scale bars*: 50 μm.

LSM510 (Carl Zeiss, Inc., Thornwood, NY, USA). All fluorescent images were generated individually using acousto-optical tunable filters to prevent cross detection of fluorophores.

Collagen Gel Contraction Assay

Cells were detached from Bioflex plates by trypsinization immediately after 24 hours of cyclical stretch. Cells were pelleted by centrifugation at 500*g* for 5 minutes. Cell pellets (2×10^5/mL) were mixed with eight volumes of rat tail type I collagen suspension, one volume of 10× concentrated DMEM, and one volume of reconstitution buffer (2% sodium bicarbonate and 4.77% HEPES dissolved in 0.05 N NaOH). The cell-populated collagen solution was immediately poured into 48-well plates (0.25 mL/well) and incubated at 37°C for 20 to 30 minutes to permit complete gelation. Collagen gels were gently released from the plates by sterile spatula and overlaid with culture media. Gel images were taken at 24 hours, and the surface area of each gel was measured using ImageJ.

Wrinkle Assay

The wrinkle assay for measurement of fibroblast contractility was performed as described in our previous studies.[30] Briefly, approximately 15 μL silicone monomer was applied onto 18-mm glass coverslips and allowed to spread for 30 minutes. The upper layer of silicone was polymerized by exposure of the coverslip to an open flame for 1.5 seconds. The silicone coverslips were placed into a 12-well plate and were equilibrated with 10 μg/mL collagen type I in serum-free DMEM media, sterilized by UV light exposure, and left overnight in the incubator at 37°C. Cells (10^4 cells/cm^2) were plated onto silicone coverslips in DMEM containing 0.1% FBS for 24 hours. Cell contraction on deformable silicone substrates was assessed by the formation of wrinkles seen with a 20 objective on a Nikon Eclipse TE 300 microscope (Nikon Instruments, Inc., Melville, NY, USA).

Statistical Analysis

Statistical differences among treatment conditions were determined using 1-way ANOVA (Newman-Keuls method for multiple comparisons). The analysis was performed with SigmaStat 3.0 software (SPSS, Inc., Chicago, IL, USA); *P* less than 0.05 was considered significant.

RESULTS

Primary ppSc Fibroblasts Isolated From Human Donor Eyes Contain an Endogenous Myofibroblast Population

Primary human ppSc fibroblasts were isolated from donor eyes using an explant approach (Fig. 1A). A total of eight ppSc fibroblast isolates were obtained from five human donor eyes,

Table 1. Primary Peripapillary Scleral (Myo)Fibroblasts Isolated From Human Donor Eyes

Age, y	Race	Sex	Cell No.	Proportion of Fully Differentiated (Myo)Fibroblasts, %
82	Caucasian	Female	1837 (OD)	11.5 ± 0.7
			1838 (OS)	25.1 ± 2.5
84	Caucasian	Female	1843 (OD)	10.6 ± 1.9
			1844 (OS)	8.0 ± 0.7
74	Caucasian	Male	1861 (OD)	10.9 ± 1.8
			1862 (OS)	18.3 ± 1.5
42	Caucasian	Male	2340 (OD)	6.2 ± 0.7
83	Caucasian	Female	1203 (OD)	47.5 ± 2.9

including three paired eyes and two unilateral (right) eyes (Table 1). The ppSc fibroblasts grown in culture present a spindle-shaped morphology of typical fibroblasts (Fig. 1B). Confocal immunofluorescent microscopy demonstrated that a subset of early-passage ppSc fibroblasts express αSMA, a marker of myofibroblasts, that further incorporates into filamentous actin (F-actin) (Fig. 1C), indicating that these cells are fully differentiated myofibroblasts.[25] The proportion of fully differentiated myofibroblasts ranges from 6.2% ± 0.7% to 47.5% ± 2.9% in the eight human ppSc fibroblast populations (Table 1). Additionally, our data show that contralateral eyes from the same human subject may contain different proportions of endogenous myofibroblasts in the peripapillary sclera.

An Increase in the Magnitude of Cyclic Strain Induces Strain Frequency-Dependent αSMA mRNA and Protein Expression in Human ppSc Fibroblasts

Human sclera is subjected to dynamic stress due to fluctuating IOP. To determine the potential effects of the magnitude and frequency of mechanical strain on human ppSc fibroblast-to-myofibroblast differentiation, eight human ppSc fibroblast isolates were subjected to 1% and 4% of equibiaxial cyclic strain at 0.05-Hz, 0.5-Hz, and 5-Hz frequencies. The strain magnitudes and frequencies used were based on our previous measurements in humans and nonhuman primates[18,27] and therefore were of physiologic relevance. We observed that 4% cyclic strain significantly increased levels of αSMA mRNA and protein as compared with 1% cyclic strain in all eight isolates of human ppSc fibroblasts at 5-Hz strain frequency (Figs. 2A–C). A significant increase in the proportion of fully differentiated myofibroblasts was observed in six ppSc fibroblast isolates (Table 2). In contrast, high-magnitude strain-induced αSMA

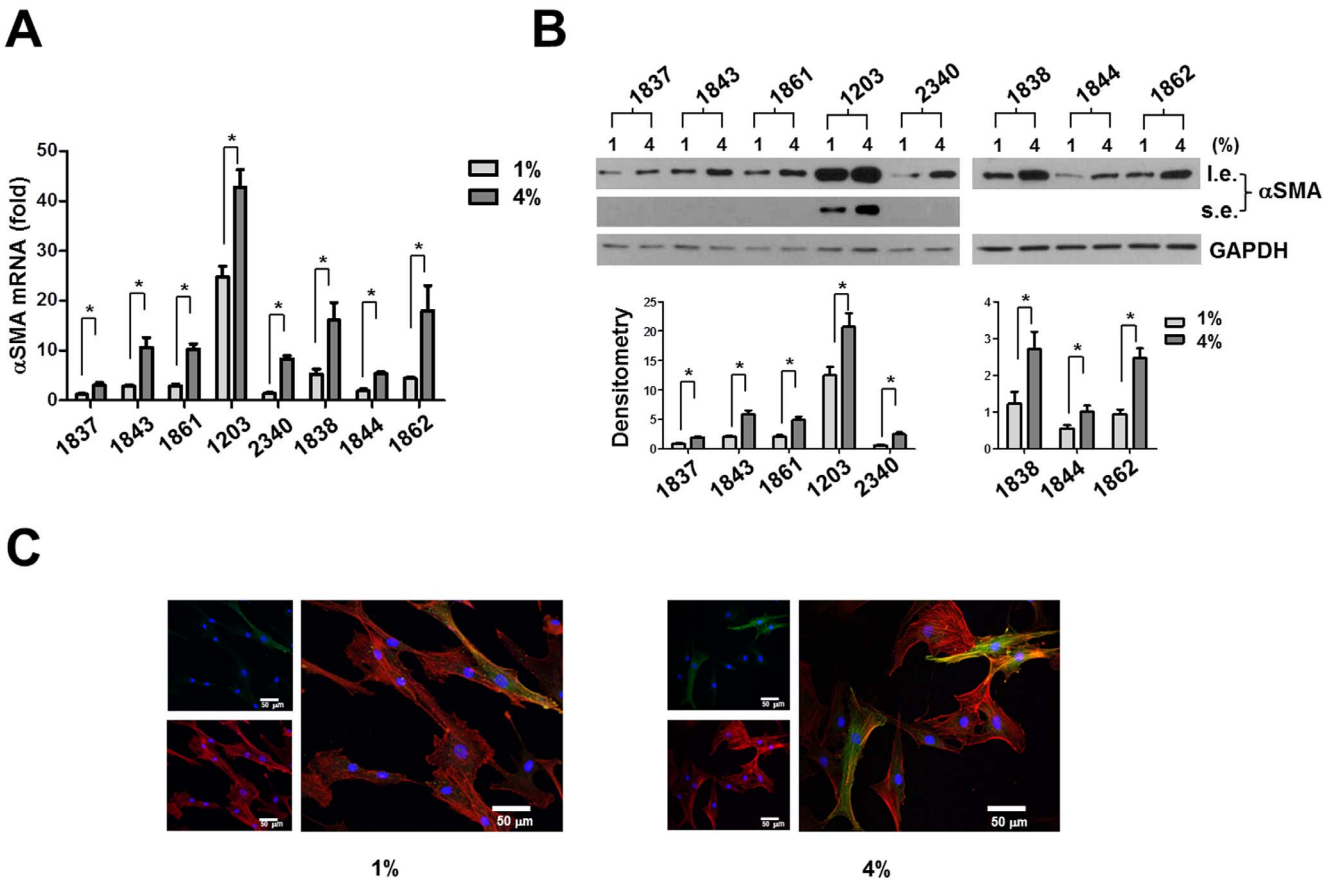

Figure 2. An increased magnitude of cyclic strain promotes αSMA mRNA and protein expression in human ppSc fibroblasts at 5-Hz strain frequency. Eight human primary ppSc fibroblast isolates were subjected to 1% or 4% cyclic strain at 5 Hz for 24 hours. (**A**) Levels of αSMA mRNA were determined by real-time PCR; 18S rRNA was used as internal control. The numerical comparative CT value obtained from No. 1837 cells at 1% strain was set to 1. (**B**) Levels of αSMA protein were determined by immunoblot. Relative levels of αSMA protein were determined by scanning densitometry of the blots and normalized to GAPDH expression. (**C**) Representative confocal immunofluorescent images showing αSMA expression (*green*) and incorporation (*yellow*) into F-actin (*red*) in ppSc myofibroblasts under 1% and 4% strain conditions. Nuclei were stained with DAPI. Results are the means ± SD of three separate experiments. $^*P < 0.05$ for comparisons as indicated. *Scale bars*: 50 μm. l.e., long exposure; s.e., short exposure.

Table 2. Proportion of Fully Differentiated ppSc (Myo)Fibroblasts Under Different Strain Conditions

ppSc (Myo)Fibroblast	No Strain, %	Strain Magnitude*	Strain Frequency, Hz, %		
			0.05	0.5	5
1837	10.7 ± 1.4	Low	12.1 ± 1.2	13.5 ± 1.7	15.9 ± 2.4†
		High	12.0 ± 1.0	14.1 ± 2.8	18.4 ± 2.2†
1838	27.3 ± 4.2	Low	25.3 ± 3.2	27.4 ± 2.9	30.2 ± 3.3†
		High	24.5 ± 2.9	27.5 ± 3.1	43.3 ± 5.3†‡
1861	11.7 ± 2.1	Low	11.5 ± 2.1	14.6 ± 2.2	16.6 ± 2.7†
		High	10.5 ± 1.4	15.2 ± 3.0†	23.2 ± 4.8†‡
1862	18.9 ± 2.7	Low	19.2 ± 3.4	21.8 ± 4.4	25.6 ± 3.5†
		High	18.3 ± 4.0	22.3 ± 3.4	36.8 ± 4.9†‡
1843	9.2 ± 1.8	Low	11.3 ± 1.2	13.4 ± 1.9	16.1 ± 2.1†
		High	10.6 ± 1.4	14.8 ± 2.0	28.0 ± 3.0†‡
1844	7.8 ± 0.6	Low	6.9 ± 0.8	10.3 ± 1.3†	12.9 ± 1.5†
		High	7.3 ± 0.5	9.8 ± 1.0	19.1 ± 2.7†‡
1203	44.3 ± 5.9	Low	48.0 ± 5.0	49.2 ± 4.8	52.2 ± 6.6
		High	47.3 ± 5.2	50.2 ± 5.4	55.5 ± 7.5
2340	7.3 ± 0.7	Low	6.4 ± 0.7	7.6 ± 0.8	10.7 ± 1.1†
		High	7.2 ± 0.4	8.7 ± 1.2	27.7 ± 2.0‡

* Low: 1%, High: 4%.
† $P < 0.05$ for comparisons between 5 Hz vs. 0.05 Hz or 0.5 Hz vs. 0.05 Hz.
‡ $P < 0.05$ for comparisons between low- versus high-strain magnitude.

mRNA and protein expression was not observed at lower strain frequencies (0.05 Hz and 0.5 Hz) (Figs. 3A–D). These data suggest that high-magnitude and high-frequency mechanical strain promotes human ppSc fibroblast-to-myofibroblast differentiation.

High-Magnitude and High-Frequency Mechanical Strain Promotes Cellular Contractility in Most Human ppSc Fibroblasts

Because acquisition of contractile activity similar to smooth muscle cells is an important characteristic of myofibroblast differentiation in addition to αSMA expression,[25] we next determined the effects of high-magnitude and high-frequency mechanical strain on human ppSc fibroblast contractility. The cell-populated collagen gel contraction assay showed that seven of eight human ppSc fibroblasts subjected to 5-Hz 4% cyclic strain had a greater reduction (shrinkage) in collagen gel surface area than cells subjected to 1% strain at the same frequency (Fig. 4A), indicating that high-magnitude and high-frequency cyclic strain promotes cellular contractility in these ppSc (myo)fibroblasts. One ppSc fibroblast isolate (No. 1203) decreased its cellular contractility in response to high-magnitude and high-frequency strain. Interestingly, this ppSc fibroblast population had the highest levels of basal αSMA mRNA and protein expression (Figs. 2, 3) and contained the largest percentage of endogenous myofibroblasts among eight human ppSc fibroblast isolates (Table 1). A single cell-based wrinkle assay demonstrated that fully differentiated myofibroblasts were contractile as evidenced by contractile force–generated wrinkle formation on silicone substrates (Fig. 4B). In contrast, αSMA-negative ppSc fibroblasts did not cause the wrinkle formation.

We previously demonstrated that MLC_{20} phosphorylation is associated with myofibroblast contractility both in vitro and in vivo.[30] Therefore, measurement of the level of phospho MLC_{20} can be used as a biochemical approach to evaluate myofibroblast contractility. Immunoblot analysis showed that high-magnitude and high-frequency cyclic strain indeed enhanced MLC_{20} phosphorylation in the seven ppSc fibroblast isolates that had increased contractility in the collagen gel assay (Fig. 4C). In contrast, the No. 1203 ppSc fibroblast isolate showed a decrease in MLC_{20} phosphorylation in response to high-magnitude and high-frequency cyclic strain.

Increasing Cyclic Strain Frequency Promotes αSMA mRNA and Protein Expression in Human ppSc Fibroblasts Under Both 1% and 4% Strain Conditions

To determine whether cyclic strain frequency regulates human ppSc fibroblast-to-myofibroblast differentiation, we compared levels of αSMA mRNA and protein in each human ppSc fibroblast isolate subjected to 0.05-Hz, 0.5-Hz, and 5-Hz cyclic strain under either 1% or 4% strain conditions. We found that increasing cyclic strain frequency promoted αSMA mRNA and protein expression in eight human ppSc fibroblast isolates under both 1% and 4% strain conditions (Figs. 5A, 5B). Higher strain frequency also significantly increased the proportions of fully differentiation myofibroblasts in most ppSc fibroblast isolates (Table 2). These data suggest that cyclic strain frequency is sufficient to regulate ppSc fibroblast-to-myofibroblast differentiation. Increasing strain frequency enhanced MLC_{20} phosphorylation in seven human ppSc fibroblast isolates at both 1% and 4% strain conditions (Fig. 5B). However, No. 1203 ppSc fibroblast isolate, which had the highest levels of αSMA expression at baseline, had an opposite response: cyclic strain with increasing frequency decreased MLC_{20} phosphorylation in this ppSc fibroblast isolate (Fig. 5B). Consistent with the previous findings (Figs. 2, 3), high-magnitude (4%) strain promoted significantly higher levels of αSMA mRNA and protein expression in ppSc fibroblasts than low-magnitude (1%) strain at 5 Hz, but not at 0.05 Hz and 0.5 Hz. Additionally, the levels of αSMA mRNA and protein at static conditions (i.e., ppSc fibroblasts were cultured in Bioflex wells but not subjected to strain) were equivalent to the levels of αSMA at 0.05 Hz strain conditions. Human ppSc (myo)fibroblasts isolated from contralateral eyes of the same donor expressed different levels of αSMA mRNA and protein (Figs. 5A, 5B).

Investigative Ophthalmology & Visual Science

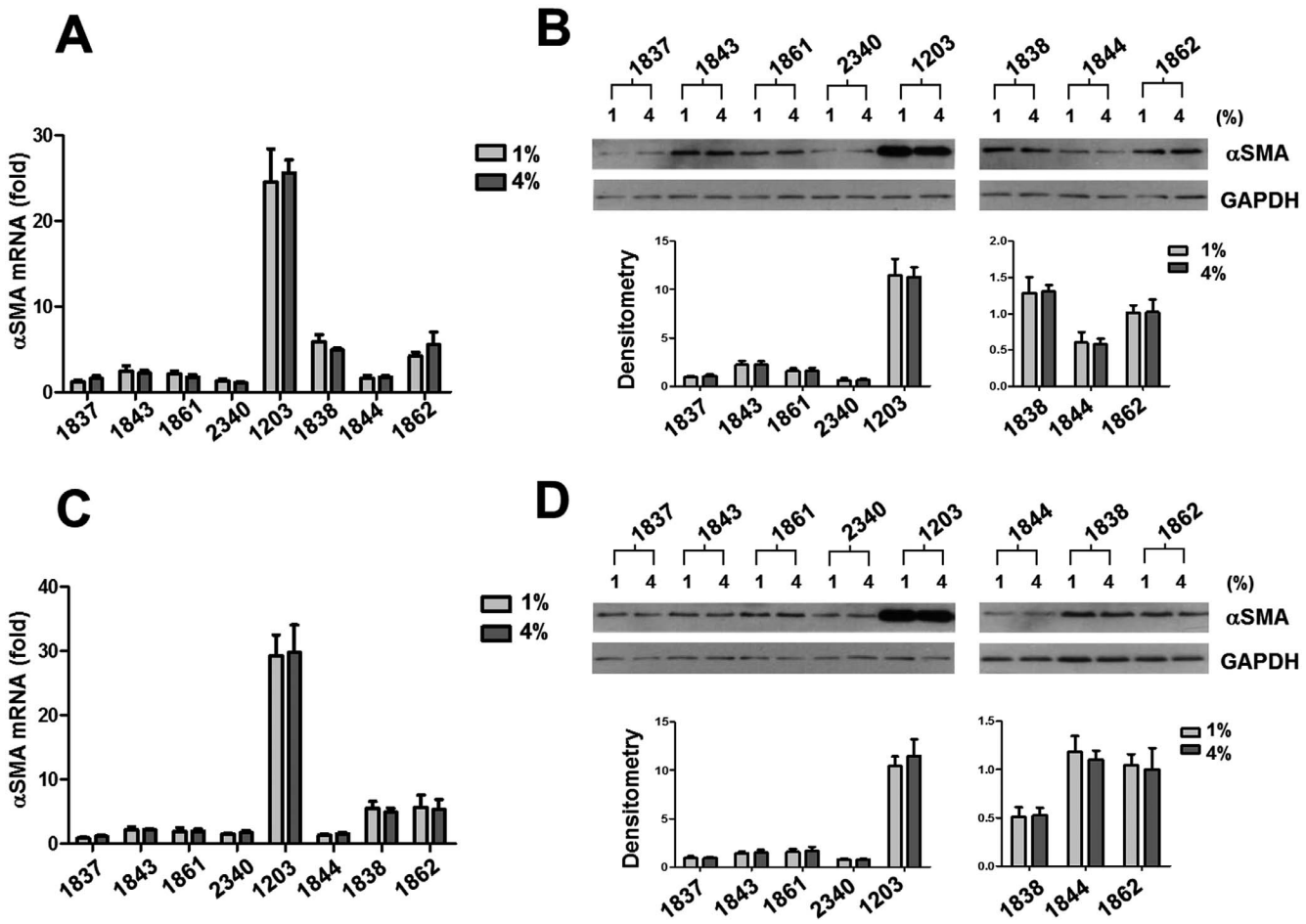

Figure 3. High-magnitude cyclic strain does not alter αSMA mRNA and protein expression in human ppSc fibroblasts at lower strain frequencies (0.05 Hz and 0.5 Hz). Eight human primary ppSc fibroblast isolates were subjected to 1% or 4% cyclic strain at 0.5 Hz (**A**, **B**) and 0.05 Hz (**C**, **D**) for 24 hours. (**A**, **C**) Levels of αSMA mRNA were determined by real-time PCR; 18S rRNA was used as internal control. The numerical comparative Ct values obtained from No. 2340 cells at 4% strain (**A**) and from No. 1837 cells at 1% strain (**C**) were set to 1, respectively. (**B**, **D**) Levels of αSMA protein were determined by immunoblot. Relative levels of αSMA protein were determined by scanning densitometry of the blots and normalized to GAPDH expression. Results are the means ± SD of three separate experiments. $^*P < 0.05$ for comparisons as indicated.

Discussion

Peripapillary scleral fibroblasts are thought to play a crucial role in posterior scleral remodeling and in regulating the biomechanical environment of the ONH under both physiologic and pathophysiologic conditions. Continuous IOP telemetry in unrestrained, awake nonhuman primates demonstrates that IOP fluctuates on a second-to-second, hour-to-hour, and day-to-day basis.[18] However, it is not known whether changes in IOP dynamics may alter the phenotype of ppSc fibroblasts, which in turn regulates scleral tissue remodeling with concomitant effects on ONH biomechanics. In this study, we demonstrated that high-magnitude and/or high-frequency mechanical strain, both within a physiologic range, are able to promote ppSc fibroblasts to differentiate into a more active myofibroblast phenotype known to be a key effector in both normal and aberrant tissue remodeling in response to injury. From the perspective of cell and matrix biology, because myofibroblasts are the primary cells responsible for connective tissue remodeling by production of ECM proteins, including proteoglycans and glycosaminoglycan (GAGs) side chains, and ECM-degrading MMPs and MMP-antagonizing TIMPs,[25] our findings suggest that the cellular constituents of ppSc may play an important role in the regulation of IOP-driven ONH biomechanics.

Myofibroblasts have both beneficial and detrimental effects on the tissue injury–repair responses. In normal would healing, wounding initiates a phenotypic transition of normal fibroblasts to form the highly contractile myofibroblasts. Myofibroblasts contract wound openings and lay down the ECM for closing the wound. Once wound closure is complete, myofibroblasts are cleared from the wound sites by several potential mechanisms, including apoptosis, senescence, and/or regression to a more quiescent state.[31–34] Thus, the promulgation of myofibroblasts at the wound sites facilitates the normal wound-healing process. However, if myofibroblasts persist at the wound sites, continuous production of the ECM proteins by these cells will lead to tissue fibrosis/scarring.[25] Importantly, myofibroblasts generate substantial contractile forces that may cause deformation of the neighboring tissues and even human diseases, such as Dupuytren's contracture.[25] Tissue fibrosis itself changes the physical properties of the connective tissues, including increased matrix stiffening.[35] Recent studies, including our own, demonstrate that stiff/fibrotic ECM promotes fibroblast proliferation, myofibroblast differentiation, and resistance to apoptosis through specific

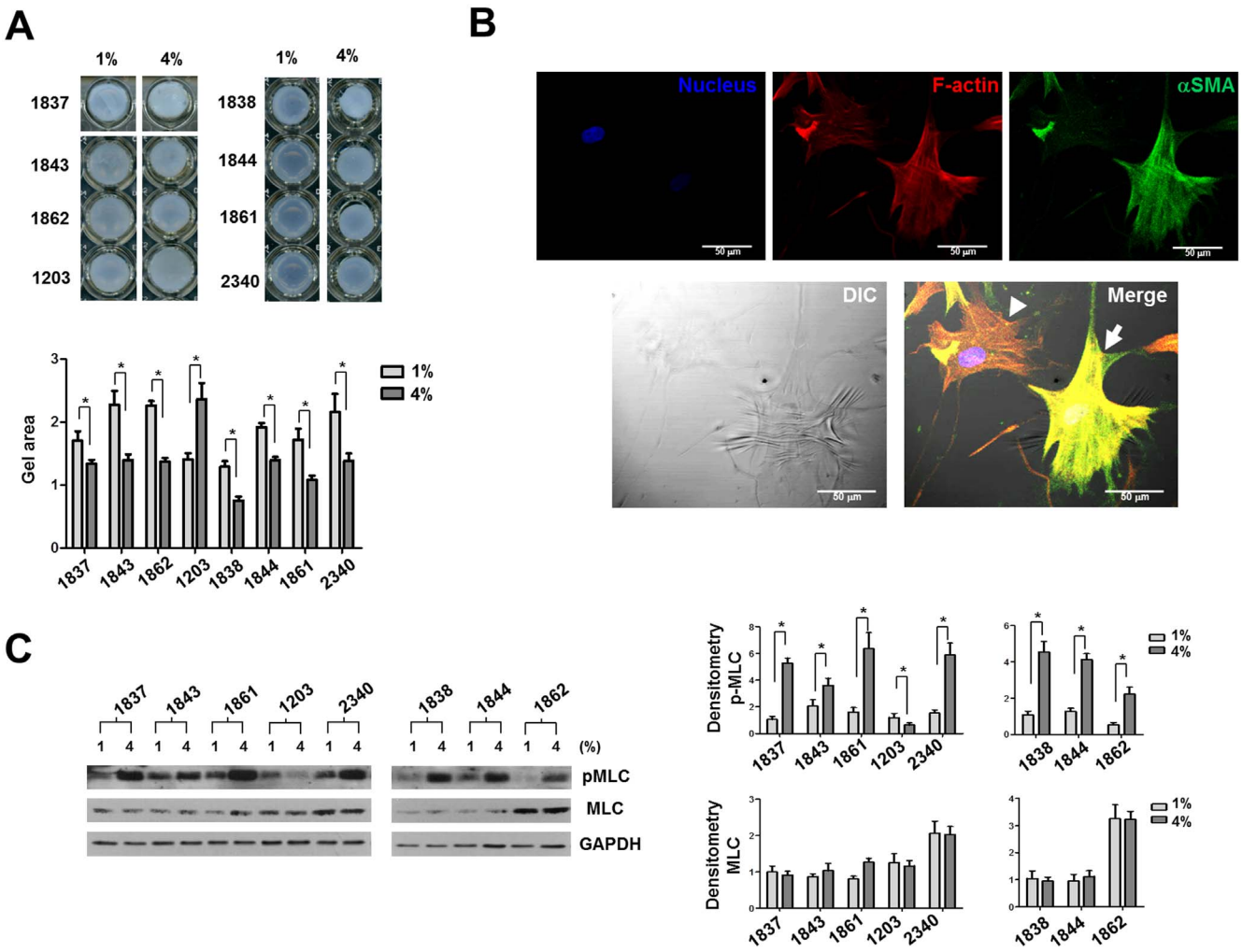

Figure 4. High-magnitude and high-frequency mechanical strain promotes cellular contractility of human ppSc fibroblasts. Eight human primary ppSc fibroblast isolates were subjected to 1% or 4% cyclic strain at 5 Hz for 24 hours. (**A**) Cells were immediately detached from BioFlex plates by trypsinization and mixed with type I collagen suspension. Fibroblast contractility was assessed by a 3D collagen gel–based assay. (**B**) The ppSc (myo)fibroblasts were cultured on silicone substrates for 24 hours. Cells were fixed and stained for αSMA (*green*) and F-actin (*red*). Nuclei were stained by DAPI (*blue*). Phase-contrast and confocal immunofluorescent images were taken and overlaid to show the correlation between αSMA expression and wrinkle formation. *Arrow* indicates a wrinkle-forming myofibroblast. *Arrowhead* indicates a non–wrinkle-forming fibroblast. *Scale bar*: 50 μm. (**C**) Levels of pMLC and total MLC_{20} (MLC) were determined by immunoblot analysis. Glyceraldehyde 3-phosphate dehydrogenase was used as loading control. Results are the means ± SD of three separate experiments. $^*P < 0.05$ for comparisons as indicated.

mechanotransduction pathways.[29,36–38] These studies suggest that sustained mechano-interactions between myofibroblasts and the connective tissues/ECM can form a positive feedback loop that perpetuates aberrant tissue remodeling. The functional role of high-magnitude and/or high-frequency strain-induced ppSc myofibroblast differentiation observed in this study is currently not clear. Based on what we have learned from both normal and aberrant tissue remodeling in other organs, it is plausible to speculate that high-magnitude and/or high-frequency strain-induced myofibroblast differentiation could be an initial protective response of ppSc fibroblasts against injurious IOP fluctuations. However, an uncontrolled expansion of the myofibroblast population might impair the mechanical homeostasis of ppSc and contribute to aberrant tissue remodeling in the glaucomatous ONH. Myofibroblasts produce collagens and develop tensile stress, which would be expected to stiffen the ppSc. Computational modeling studies suggest that stiffer sclera protects the ONH against biomechanical insults.[15,39,40] In contrast, it has been reported that having a stiffer sclera may actually accelerate damage to the axons of retinal ganglion cells.[41] Stiffening of the scleral shell leads to greater high-frequency IOP fluctuations.[18,42] A growing body of research has shown that the sclera becomes stiffer in glaucoma.[7,43,44] These latter findings would support a link between myofibroblast-mediated detrimental sclera remodeling and mechanical damage to the ONH.

Expression of αSMA and incorporation into actin stress fibers are associated with myofibroblast acquisition of contractile activities.[45] In this study, we found that one ppSc fibroblast isolate (No. 1203) expressed higher levels of αSMA than other ppSc fibroblasts at baseline (Fig. 5). High-magnitude and/or high-frequency mechanical strain further increased αSMA expression in this cell population (Fig. 2B). Despite higher levels of αSMA expression, the collagen gel contraction assay showed that No. 1203 ppSc fibroblasts had contractile activities similar to other ppSc fibroblasts. Surprisingly, No. 1203 ppSc fibroblasts showed a decrease, rather than an increase, in contractility in response to high-magnitude and

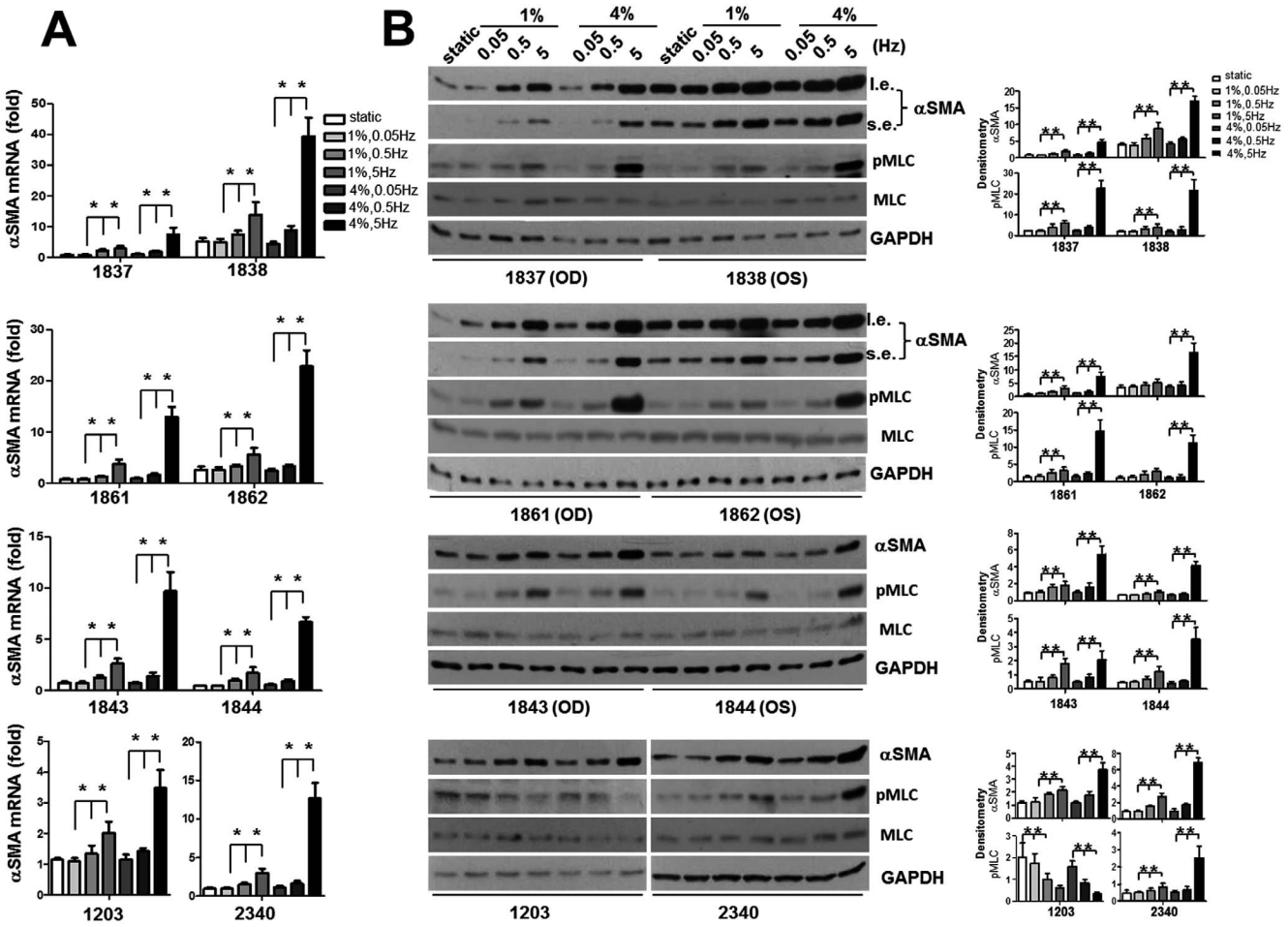

FIGURE 5. Increasing strain frequency is sufficient to promote human ppSc myofibroblast differentiation. Eight human primary ppSc fibroblast isolates were subjected to 1% or 4% cyclic strain at 0.05 Hz, 0.5 Hz, or 5Hz for 24 hours. (**A**) Levels of αSMA mRNA were determined by real-time PCR; 18S rRNA was used as internal control. The numerical comparative CT values obtained from No. 1837 cells at 4%, 0.05 Hz strain, No. 1861 cells at static condition, No. 1844 cells at 1%, 0.5 Hz stain, and No. 1203 cells at 1%, 0.05 Hz stain were set to 1, respectively. (**B**) Levels of αSMA, phosphorylated MLC_{20} and total MLC_{20} were determined by immunoblot. Glyceraldehyde 3-phosphate dehydrogenase was used as loading control. Results are the means ± SD of three separate experiments. $^{*}P < 0.05$ for comparisons as indicated. OS and OD indicate paired eyes.

high-frequency mechanical strain (Fig. 4A). The precise mechanisms by which αSMA expression decouples myofibroblast contractility in this cell population remains to be determined. However, we found that high-magnitude and/or high-frequency strain decreased MLC_{20} phosphorylation in No. 1203 ppSc fibroblasts, which is in contrast to increases in both αSMA expression and MLC_{20} phosphorylation in the other seven ppSc fibroblasts when they were subjected to high-magnitude and/or high-frequency strain (Figs. 4B, 5B). This suggests that αSMA expression alone may not be sufficient for myofibroblasts to generate contractile forces. The MLC_{20} is a regulatory subunit located on the myosin heads. Phosphorylation of MLC_{20} by increased myosin light chain kinase activity and/or decreased myosin light chain phosphatase activity lead to cross-bridge formation between the myosin heads and the actin filaments, resulting in myofibroblast contraction.[25] Our findings suggest that inhibition of MLC_{20} phosphorylation in No. 1203 cells may be associated with decreased cellular contractility in response to high-magnitude and/or high-frequency strain. However, these findings raise an additional interesting question of why No. 1203 ppSc fibroblasts are protected from high-magnitude and high-frequency mechanical strain–induced cellular contraction. Our current hypothesis is that this might be a protective mechanism for the ppSc that inherently processes a high percentage of endogenous myofibroblasts. When this kind of ppSc experiences mechanical insults, disabling of myofibroblasts from generating excessive contractile forces would not only protect cells themselves, but prevent overproduction of mechanical tension in the local environment, thus maintaining the mechanical homeostasis of the ppSc as well as ONH.

The current study has several limitations. First, as very little is known about IOP fluctuations in humans, the strain frequencies used in this study were based on IOP measurements in nonhuman primates.[18] In addition, studies from monkeys reveal that IOP fluctuates in disparate patterns,[18] whereas the Flexcell tension system applies monotonous stretch cycles to cells. The experimental results obtained in this study will need to be validated under variable cyclic stretch that incorporates physiological levels of cycle-by-cycle variability experienced by human ppSc fibroblasts in vivo. Second, the current study did not include ppSc fibroblasts isolated from patients with glaucoma. Comparisons of normal versus glaucomatous ppSc fibroblasts for the proportion of endogenous myofibroblast populations and the responses to various mechanical strains will provide important insights to

understand the role of the cellular constituent of ppSc in the regulation of ONH biomechanics and glaucomatous optic neuropathy. Last, we did not address the mechanotransduction mechanisms by which high-magnitude and/or high-frequency mechanical strain promotes ppSc myofibroblast differentiation. Identification of key mechanotransduction pathways in this process might provide novel molecular targets for amelioration of deleterious mechanical insults and will be the focus of future investigations.

In summary, this study provides evidence that human ppSc fibroblasts are mechanosensitive cells that are able to respond to altered mechanical strains with a phenotypic transition into myofibroblasts, a type of specialized contractile cell known to have both beneficial and detrimental effects in the tissue-remodeling process. These findings suggest that the cellular constituent of ppSc may play an active and ever-changing role in the regulation of both the mechanobiology and the mechanopathobiology of the ONH.

Acknowledgments

The authors thank the Alabama Eye Bank for procurement of eyes from human donors, Rafael Grytz, PhD, Massimo A. Fazio, PhD, and Joel Berry, PhD, for helpful discussions, and Lan Wang, MD, for her technical assistance with eye dissection.

Supported in part by the EyeSight Foundation of Alabama, Research to Prevent Blindness (YZ), National Institutes of Health Grants HL124076 (YZ) and EY018926 (JCD/CAG), American Heart Association Grant-in-Aid 14GRNT2018023 (YZ), and American Thoracic Society Recognition Award (YZ).

Disclosure: **J. Qu**, None; **H. Chen**, None; **L. Zhu**, None; **N. Ambalavanan**, None; **C.A. Girkin**, None; **J.E. Murphy-Ullrich**, None; **C. Downs**, None; **Y. Zhou**, None

References

1. Burgoyne CF, Downs JC, Bellezza AJ, Suh JK, Hart RT. The optic nerve head as a biomechanical structure: a new paradigm for understanding the role of IOP-related stress and strain in the pathophysiology of glaucomatous optic nerve head damage. *Prog Retin Eye Res*. 2005;24:39–73.
2. Downs JC. Optic nerve head biomechanics in aging and disease. *Exp Eye Res*. 2015;133:19–29.
3. Campbell IC, Coudrillier B, Ross Ethier C. Biomechanics of the posterior eye: a critical role in health and disease. *J Biomech Eng*. 2014;136:021005.
4. Sigal IA, Ethier CR. Biomechanics of the optic nerve head. *Exp Eye Res*. 2009;88:799–807.
5. Cone-Kimball E, Nguyen C, Oglesby EN, Pease ME, Steinhart MR, Quigley HA. Scleral structural alterations associated with chronic experimental intraocular pressure elevation in mice. *Mol Vis*. 2013;19:2023–2039.
6. Downs JC, Roberts MD, Burgoyne CF. Mechanical environment of the optic nerve head in glaucoma. *Optom Vis Sci*. 2008;85:425–435.
7. Coudrillier B, Tian J, Alexander S, Myers KM, Quigley HA, Nguyen TD. Biomechanics of the human posterior sclera: age- and glaucoma-related changes measured using inflation testing. *Invest Ophthalmol Vis Sci*. 2012;53:1714–1728.
8. Pijanka JK, Coudrillier B, Ziegler K, et al. Quantitative mapping of collagen fiber orientation in non-glaucoma and glaucoma posterior human sclerae. *Invest Ophthalmol Vis Sci*. 2012;53:5258–5270.
9. Quigley HA, Brown A, Dorman-Pease ME. Alterations in elastin of the optic nerve head in human and experimental glaucoma. *Br J Ophthalmol*. 1991;75:552–557.
10. Quigley HA, Dorman-Pease ME, Brown AE. Quantitative study of collagen and elastin of the optic nerve head and sclera in human and experimental monkey glaucoma. *Curr Eye Res*. 1991;10:877–888.
11. Downs JC, Ensor ME, Bellezza AJ, Thompson HW, Hart RT, Burgoyne CF. Posterior scleral thickness in perfusion-fixed normal and early-glaucoma monkey eyes. *Invest Ophthalmol Vis Sci*. 2001;42:3202–3208.
12. Yang H, Downs JC, Girkin C, et al. 3-D histomorphometry of the normal and early glaucomatous monkey optic nerve head: lamina cribrosa and peripapillary scleral position and thickness. *Invest Ophthalmol Vis Sci*. 2007;48:4597–4607.
13. Sigal IA, Yang H, Roberts MD, et al. IOP-induced lamina cribrosa deformation and scleral canal expansion: independent or related? *Invest Ophthalmol Vis Sci*. 2011;52:9023–9032.
14. Grytz R, Meschke G, Jonas JB. The collagen fibril architecture in the lamina cribrosa and peripapillary sclera predicted by a computational remodeling approach. *Biomech Model Mechanobiol*. 2011;10:371–382.
15. Norman RE, Flanagan JG, Sigal IA, Rausch SM, Tertinegg I, Ethier CR. Finite element modeling of the human sclera: influence on optic nerve head biomechanics and connections with glaucoma. *Exp Eye Res*. 2011;93:4–12.
16. Coudrillier B, Boote C, Quigley HA, Nguyen TD. Scleral anisotropy and its effects on the mechanical response of the optic nerve head. *Biomech Model Mechanobiol*. 2013;12:941–963.
17. Burgoyne CF. A biomechanical paradigm for axonal insult within the optic nerve head in aging and glaucoma. *Exp Eye Res*. 2011;93:120–132.
18. Downs JC, Burgoyne CF, Seigfreid WP, Reynaud JF, Strouthidis NG, Sallee V. 24-hour IOP telemetry in the nonhuman primate: implant system performance and initial characterization of IOP at multiple timescales. *Invest Ophthalmol Vis Sci*. 2011;52:7365–7375.
19. Shelton L, Rada JS. Effects of cyclic mechanical stretch on extracellular matrix synthesis by human scleral fibroblasts. *Exp Eye Res*. 2007;84:314–322.
20. Smith JD, Hamir AN, Greenlee JJ. Cartilaginous metaplasia in the sclera of Suffolk sheep. *Vet Pathol*. 2011;48:827–829.
21. Phillips JR, McBrien NA. Pressure-induced changes in axial eye length of chick and tree shrew: significance of myofibroblasts in the sclera. *Invest Ophthalmol Vis Sci*. 2004;45:758–763.
22. Hinz B, Phan SH, Thannickal VJ, Galli A, Bochaton-Piallat ML, Gabbiani G. The myofibroblast: one function, multiple origins. *Am J Pathol*. 2007;170:1807–1816.
23. Poukens V, Glasgow BJ, Demer JL. Nonvascular contractile cells in sclera and choroid of humans and monkeys. *Invest Ophthalmol Vis Sci*. 1998;39:1765–1774.
24. Backhouse S, Phillips JR. Effect of induced myopia on scleral myofibroblasts and in vivo ocular biomechanical compliance in the guinea pig. *Invest Ophthalmol Vis Sci*. 2010;51:6162–6171.
25. Tomasek JJ, Gabbiani G, Hinz B, Chaponnier C, Brown RA. Myofibroblasts and mechano-regulation of connective tissue remodelling. *Nat Rev Mol Cell Biol*. 2002;3:349–363.
26. Hinz B, Phan SH, Thannickal VJ, et al. Recent developments in myofibroblast biology: paradigms for connective tissue remodeling. *Am J Pathol*. 2012;180:1340–1355.
27. Fazio MA, Grytz R, Morris JS, et al. Age-related changes in human peripapillary scleral strain. *Biomech Model Mechanobiol*. 2014;13:551–563.
28. Huang X, Yang N, Fiore VF, et al. Matrix stiffness-induced myofibroblast differentiation is mediated by intrinsic mechanotransduction. *Am J Respir Cell Mol Biol*. 2012;47:340–348.

29. Zhou Y, Huang X, Hecker L, et al. Inhibition of mechanosensitive signaling in myofibroblasts ameliorates experimental pulmonary fibrosis. *J Clin Invest*. 2013;123:1096–1108.
30. Huang X, Gai Y, Yang N, et al. Relaxin regulates myofibroblast contractility and protects against lung fibrosis. *Am J Pathol*. 2011;179:2751–2765.
31. Kisseleva T, Cong M, Paik Y, et al. Myofibroblasts revert to an inactive phenotype during regression of liver fibrosis. *Proc Natl Acad Sci U S A*. 2012;109:9448–9453.
32. Desmoulière A, Redard M, Darby I, Gabbiani G. Apoptosis mediates the decrease in cellularity during the transition between granulation tissue and scar. *Am J Pathol*. 1995;146:56–66.
33. Krizhanovsky V, Yon M, Dickins RA, et al. Senescence of activated stellate cells limits liver fibrosis. *Cell*. 2008;134:657–667.
34. Grinnell F, Zhu M, Carlson MA, Abrams JM. Release of mechanical tension triggers apoptosis of human fibroblasts in a model of regressing granulation tissue. *Exp Cell Res*. 1999;248:608–619.
35. Hinz B. Matrix mechanics and regulation of the fibroblast phenotype. *Periodontol 2000*. 2013;63:14–28.
36. Liu F, Mih JD, Shea BS, et al. Feedback amplification of fibrosis through matrix stiffening and COX-2 suppression. *J Cell Biol*. 2010;190:693–706.
37. Huang X, Yang N, Fiore VF, et al. Matrix stiffness-induced myofibroblast differentiation is mediated by intrinsic mechanotransduction. *Am J Respir Cell Mol Biol*. 2012;47:340–348.
38. Rahaman SO, Grove LM, Paruchuri S, et al. TRPV4 mediates myofibroblast differentiation and pulmonary fibrosis in mice. *J Clin Invest*. 2014;124:5225–5238.
39. Sigal IA, Flanagan JG, Ethier CR. Factors influencing optic nerve head biomechanics. *Invest Ophthalmol Vis Sci*. 2005;46:4189–4199.
40. Eilaghi A, Flanagan JG, Simmons CA, Ethier CR. Effects of scleral stiffness properties on optic nerve head biomechanics. *Ann Biomed Eng*. 2010;38:1586–1592.
41. Kimball EC, Nguyen C, Steinhart MR, et al. Experimental scleral cross-linking increases glaucoma damage in a mouse model. *Exp Eye Res*. 2014;128:129–140.
42. Morris HJ, Tang J, Cruz Perez B, et al. Correlation between biomechanical responses of posterior sclera and IOP elevations during micro intraocular volume change. *Invest Ophthalmol Vis Sci*. 2013;54:7215–7222.
43. Hommer A, Fuchsjäger-Mayrl G, Resch H, Vass C, Garhofer G, Schmetterer L. Estimation of ocular rigidity based on measurement of pulse amplitude using pneumotonometry and fundus pulse using laser interferometry in glaucoma. *Invest Ophthalmol Vis Sci*. 2008;49:4046–4050.
44. Nguyen C, Cone FE, Nguyen TD, et al. Studies of scleral biomechanical behavior related to susceptibility for retinal ganglion cell loss in experimental mouse glaucoma. *Invest Ophthalmol Vis Sci*. 2013;54:1767–1780.
45. Hinz B, Celetta G, Tomasek JJ, Gabbiani G, Chaponnier C. Alpha-smooth muscle actin expression upregulates fibroblast contractile activity. *Mol Biol Cell*. 2001;12:2730–2741.

Investigative Ophthalmology & Visual Science